© 2015. Published by The Company of Biologists Ltd | Journal of Cell Science (2015) 128, 1308–1315 doi:10.1242/jcs.156737

RESEARCH ARTICLE

Loss of BMPR2 leads to high bone mass due to increased osteoblast activity

Jonathan W. Lowery[1,2], Giuseppe Intini[3], Laura Gamer[2], Sutada Lotinun[3,4], Valerie S. Salazar[2], Satoshi Ote[2], Karen Cox[2], Roland Baron[3] and Vicki Rosen[2,*]

ABSTRACT

Imbalances in the ratio of bone morphogenetic protein (BMP) versus activin and TGFβ signaling are increasingly associated with human diseases yet the mechanisms mediating this relationship remain unclear. The type 2 receptors ACVR2A and ACVR2B bind BMPs and activins but the type 2 receptor BMPR2 only binds BMPs, suggesting that type 2 receptor utilization might play a role in mediating the interaction of these pathways. We tested this hypothesis in the mouse skeleton, where bone mass is reciprocally regulated by BMP signaling and activin and TGFβ signaling. We found that deleting *Bmpr2* in mouse skeletal progenitor cells (*Bmpr2*-cKO mice) selectively impaired activin signaling but had no effect on BMP signaling, resulting in an increased bone formation rate and high bone mass. Additionally, activin sequestration had no effect on bone mass in *Bmpr2*-cKO mice but increased bone mass in wild-type mice. Our findings suggest a novel model whereby BMPR2 availability alleviates receptor-level competition between BMPs and activins and where utilization of ACVR2A and ACVR2B by BMPs comes at the expense of activins. As BMP and activin pathway modulation are of current therapeutic interest, our findings provide important mechanistic insight into the relationship between these pathways in human health.

KEY WORDS: BMP, Activin, BMPR2, Bone mass, Osteoblast, Osteoporosis

INTRODUCTION

All TGFβ superfamily cytokines [BMPs, GDFs, activin and activin-like ligands, such as GDF8 (also known as myostatin) and GDF11 (hereafter collectively referred to as 'activins' for simplicity), and TGFβ] can be categorized based on their activation of one of two distinct downstream pathways – either through SMAD1, SMAD5 and SMAD8 (hereafter denoted as SMAD1/5/8; note that SMAD8 is also known as SMAD9) or SMAD2 and SMAD3 (hereafter denoted as SMAD2/3), which are the canonical BMP signaling and activin and TGFβ signaling effectors, respectively (Lowery and de Caestecker, 2010). The canonical BMP pathway and activin and TGFβ pathway antagonize one another in numerous physiological contexts, including in early embryonic development, where SMAD2 antagonizes SMAD1 to establish body patterning (Yamamoto et al., 2009), in angiogenesis, where the balance of SMAD1/5/8 and SMAD2/3 establishes an angiogenic switch between activation and resolution phases (Goumans et al., 2003), in cell fate of type 2 alveolar epithelial cells, where trans-differentiation to a type 1 alveolar program is promoted by SMAD2/3, but restricted by SMAD1/5/8 (Zhao et al., 2013), during maintenance of epithelial cell polarity, where SMAD1/5/8 restricts the TGFβ-induced epithelial–mesenchymal transition (Saitoh et al., 2013), and during regulation of skeletal muscle mass, where SMAD1/5/8 and SMAD2/3 signaling inversely impact on muscle hypertrophy (Sartori et al., 2013; Winbanks et al., 2013). Moreover, imbalances in the ratio of TGFβ superfamily cytokines are increasingly associated with human diseases, including pulmonary and kidney fibrosis (Izumi et al., 2006; Nguyen and Goldschmeding, 2008), glaucoma (Wordinger et al., 2007; Zode et al., 2009), asthma (Stumm et al., 2014) and pulmonary arterial hypertension (Han et al., 2013; Morrell et al., 2001). However, the mechanisms that allow the BMP pathway and the activin and TGFβ pathway to antagonize one another remain unclear. For instance, competition for the shared transcription factor SMAD4 (Candia et al., 1997; Sartori et al., 2013) and regulation of downstream target genes (Oshimori and Fuchs, 2012) are likely insufficient general explanations because SMAD4, which is common to both pathways, is not always limiting (Piek et al., 1999) and target genes vary greatly by biological context (Massagué, 2012). Less attention has been paid, however, to potential regulation at the level of pathway activation via receptor utilization, which could influence the ratio of signaling upstream of any additional mechanisms.

TGFβ superfamily ligands signal through heteromeric combinations of type 1 and type 2 receptors, and both receptor types are essential to elicit downstream signaling. BMPs, activins and TGFβs generally utilize separate type 1 receptors (Hinck, 2012). In contrast, TGFβ has a unique type 2 receptor, whereas the type 2 receptors ACVR2A and ACVR2B (hereafter denoted ACVR2A/B) bind activins with high affinity but also bind BMPs with comparatively lower affinity. BMPs therefore can utilize ACVR2A/B and also the BMP-specific type 2 receptor, BMPR2, allowing for potential competition for ACVR2A/B by BMPs and activin based on the availability of BMPR2. We examined this hypothesis in the context of the mouse skeleton, taking advantage of the fact that postnatal bone formation and mineralization is under tight reciprocal regulation by BMPs and activins (Alves et al., 2013; Eijken et al., 2007; Fajardo et al., 2010; Ikenoue et al., 1999; Koncarevic et al., 2010; Li et al., 2013; Lotinun et al., 2010; Matsumoto et al., 2012; Mishina et al., 2004; Nicks et al.,

[1]Department of Biomedical Science, Marian University College of Osteopathic Medicine, Indianapolis, IN 46222, USA. [2]Department of Developmental Biology, Harvard School of Dental Medicine, Boston, MA 02115, USA. [3]Department of Oral Medicine, Infection, and Immunity, Harvard School of Dental Medicine, Boston, MA 02115, USA. [4]Department of Physiology, Faculty of Dentistry, Chulalongkorn University, Bangkok, 10330, Thailand.

*Author for correspondence (Vicki_Rosen@hsdm.harvard.edu)

Received 19 May 2014; Accepted 2 February 2015

Journal of Cell Science

Journal of Cell Science (2015) 128, 1308–1315 doi:10.1242/jcs.156737

2009; Pearsall et al., 2008; Perrien et al., 2007; Ruckle et al., 2009; Sakai et al., 2000; Sherman et al., 2013; Simic et al., 2006; Zhang et al., 2009; Zhao et al., 2002). Surprisingly, engineering specific deletion of BMPR2 in bone-forming cells (*Bmpr2*-cKO mice) selectively reduces activin pathway activation but has no apparent effect on BMP signaling. Additionally, *Bmpr2*-cKO mice develop substantially higher bone mass and bone mineral density by 9 weeks of age due to a higher bone formation rate, which is consistent with impaired activin signaling (Alves et al., 2013; Eijken et al., 2007; Ikenoue et al., 1999; Perrien et al., 2007). Our findings suggest a novel model whereby availability of BMPR2 in target cells permits partial segregation of ACVR2A/B to the activin pathway and increased BMP utilization of ACVR2A/B comes at the expense of activin signaling.

RESULTS

Type 2 BMP and activin receptor expression in bone cells

Each of the type 2 receptors *Bmpr2*, *Acvr2a* and *Acvr2b* are expressed in the postnatal skeleton (Fig. 1A; Liu et al., 2012). To remove BMPR2 from bone-forming cells, we crossed *Bmpr2*$^{floxed/floxed}$ mice to Paired-related homeobox gene 1 (*Prx1*)-Cre transgenic mice (Logan et al., 2002), which accomplishes widespread recombination and subsequent permanent loss of BMPR2 in osteoprogenitors, osteoblasts and osteocytes of the limb skeleton (Almeida et al., 2013; Logan et al., 2002). Loss of full-length BMPR2 in *Bmpr2*-cKO; *Prx1*-Cre mice (*Bmpr2*-cKO mice) was confirmed at the mRNA and protein levels (Gamer et al., 2011). Importantly, the bone-specific expression levels of *Acvr2a* and *Acvr2b* are unchanged in the bones of *Bmpr2*-cKO mice (Fig. 1B,C; Gamer et al., 2011).

Removal of BMPR2 selectively reduces activated SMAD2/3 in bone cells

We next performed western blots on marrow-free femora lysates to investigate whether signaling changes are associated with loss of BMPR2 expression and found that the level of phosphorylated (i.e. activated) SMAD1/5/8 was unchanged in *Bmpr2*-cKO mice at 4 weeks and 9 weeks of age (supplementary material Fig. S1A; Fig. 1D). Given that type 2 receptor occupancy is required for BMP signaling, ACVR2A/B appear to functionally compensate for loss of BMPR2 in bone cells *in vivo*. To examine whether this shift in receptor usage by BMPs has an effect on activin signaling, we next evaluated the level of phosphorylated (i.e. activated) SMAD2/3. Whereas activated SMAD2/3 was unaffected in *Bmpr2*-cKO mice at 4 weeks of age (supplementary material Fig. S1A), the level of activated SMAD2/3 was substantially reduced in *Bmpr2*-cKO mice at 9 weeks of age (Fig. 1E).

To examine, in a cell-specific manner, whether reduced SMAD2/3 activation is directly related to loss of BMPR2, we isolated primary osteoblasts from *Bmpr2*-floxed mice, which express each of the type 2 receptors *Bmpr2*, *Acvr2a* and *Acvr2b* (Fig. 2A), and induced recombination using adenoviral delivery of *Cre*. Loss of full-length BMPR2 was confirmed at the mRNA (Fig. 2B) and protein (Fig. 2C) levels. Consistent with our results in femora lysates, the basal level of canonical activin and TGFβ signaling was reduced, whereas canonical BMP signaling was unaffected in *Bmpr2*-cKO osteoblasts (Fig. 2C,D). This does not appear to be due to decreased activin ligand availability given that expression levels of the activin subunits *Inhba* and *Inhbb* and the antagonists inhibin α (*Inha*) and follistatin were unchanged in *Bmpr2*-cKO osteoblasts (supplementary material Fig. S2A). Note that because *Bmpr2*-cKO osteoblasts were responsive to exogenous activin A (supplementary material Fig. S2B), reduced basal SMAD2/3 activation in this cell population is not due to a requirement for BMPR2 in activin signaling.

High bone mass in *Bmpr2*-cKO mice due to an increased bone formation rate

We next examined the impact of loss of BMPR2 on postnatal bone physiology *in vivo*. Although limb skeletogenesis and expression of bone markers are unchanged in *Bmpr2*-cKO mice at birth (Gamer et al., 2011) and at 4 weeks of age (supplementary material Fig. S3A), both male and female *Bmpr2*-cKO mice display high trabecular bone mass and increased bone mineral

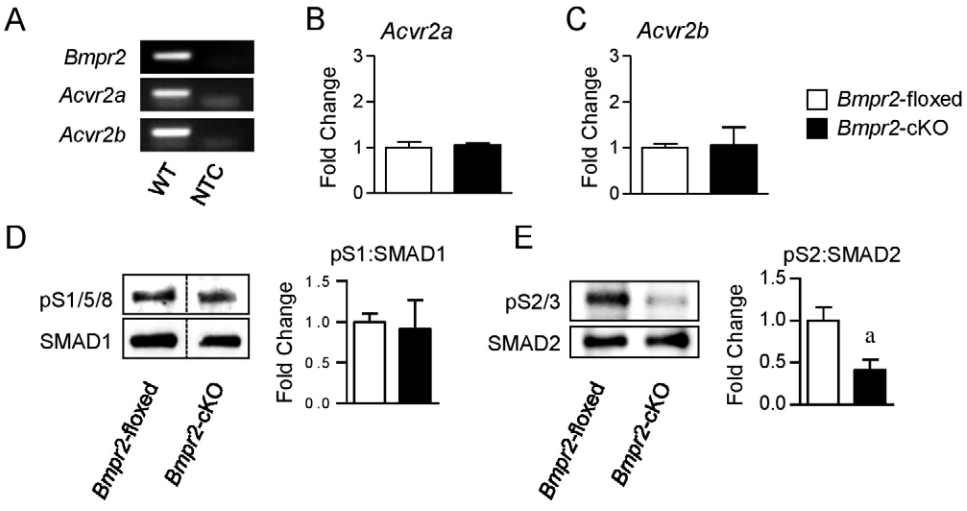

Fig. 1. Effects of removing *Bmpr2* in bone. (A) RT-PCR for *Bmpr2*, *Acvr2a*, and *Acvr2b* expression in wild-type (WT) 15-week-old mouse humerus. NTC, no DNA template control. (B,C) Expression of *Acvr2a* (B) and *Acvr2b* (C) in humerii of 4-week-old *Bmpr2*-cKO mice compared to *Bmpr2*-floxed littermates ($n \geq 4$ per genotype). (D,E) Western blots for phosphorylated isoforms of SMAD1/5/8 (pS1/5/8) and SMAD2/3 (pS2/3) relative to total SMAD1 or SMAD2. Lysates are from marrow-free femora of female mice at 9 weeks of age. Densitometry are normalized to *Bmpr2*-floxed from $n=3$ each genotype. $^{a}P<0.05$ compared with *Bmpr2*-floxed. The vertical bar in D indicates removal of intervening lane so that samples most representative of group mean are shown; the blot image with the intervening lane present is shown in supplementary material Fig. S1B.

Journal of Cell Science (2015) 128, 1308–1315 doi:10.1242/jcs.156737

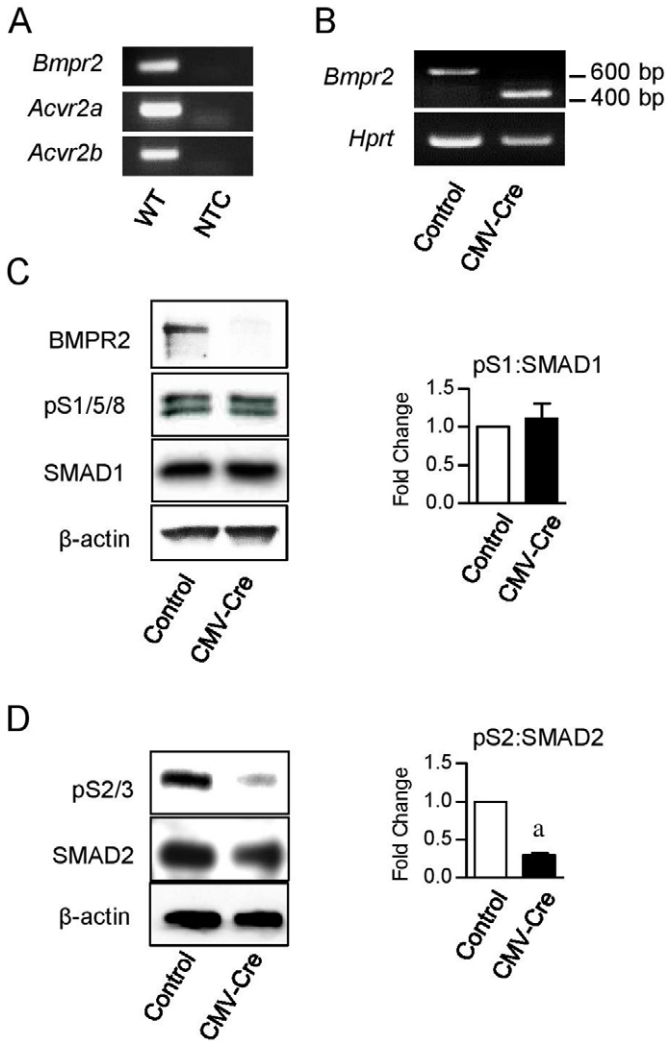

Fig. 2. Reduced activated SMAD2/3 in *Bmpr2*-cKO osteoblasts. (A) RT-PCR for *Bmpr2*, *Acvr2a* and *Acvr2b* expression in *Bmpr2*-floxed (WT) osteoblasts. NTC, no DNA template control. (B–E) Loss of full-length *Bmpr2* after adenoviral CMV-Cre delivery was confirmed at the mRNA level (B) by RT-PCR and protein level (C) by western blotting. Western blots for phosphorylated isoforms of SMAD1/5/8 (C, pS1/5/8) and SMAD2/3 (D, pS2/3) relative to total SMAD1 or SMAD2. Densitometry (graphs on the right) represents three independent isolation and transduction experiments normalized to control. *Hprt* and β-actin serve as loading controls in B, and C and D, respectively. [a]$P<0.002$ compared with control by paired Student's *t*-test.

density in the tibia by 9 weeks of age (Table 1; Fig. 3A). As an internal control, we examined the L5 vertebrae of *Bmpr2*-cKO mice (supplementary material Table S1), which is outside the *Prx1*-Cre expression domain. Bone mass is unaffected at this site, confirming that increased tibial bone mass is specifically due to Cre-dependent loss of *Bmpr2*.

We then performed detailed histomorphometric analyses (Dempster et al., 2013) to examine the cellular mechanism(s) responsible for the high bone mass in *Bmpr2*-cKO mice. Whereas osteoblast density and coverage of individual bone surfaces were unchanged in *Bmpr2*-cKO mice (Table 2), *in vivo* calcein labeling indicated that the percentage of bone surface undergoing mineralization tended to be higher in *Bmpr2*-cKO mice during the labeling period of 9 and 10 weeks of age. Bone mineral apposition rate was also significantly increased at this time (Table 2), resulting in a substantially elevated bone formation rate (Fig. 3B; Table 2). Although *Prx1*-Cre is not expressed in osteoclasts (Almeida et al., 2013; Kolanczyk et al., 2007), we examined whether *Bmpr2*-cKO mice displayed secondary defects in bone resorption. Osteoclast density, osteoclast coverage, and the percentage bone surface undergoing resorption were unchanged in *Bmpr2*-cKO mice (Table 2). Furthermore, the increase in bone volume in *Bmpr2*-cKO mice was proportional to the elevation in bone formation rate (Fig. 3C), indicating that bone resorption is unaffected by loss of BMPR2 in bone-forming cells.

Collectively, these findings indicate that the high bone mass we observe in in *Bmpr2*-cKO mice is due to increased individual osteoblast activity coincident with bone-specific reduction in activin signaling.

Activin sequestration has no effect on bone mass in *Bmpr2*-cKO mice

Our results led us to hypothesize that impaired activin signaling is responsible for the high bone mass seen in *Bmpr2*-cKO mice. We tested this idea by treating *Bmpr2*-floxed and *Bmpr2*-cKO mice with ACVR2B receptor decoy (ACVR2B-Fc), which sequesters activins with high affinity (Koncarevic et al., 2012; Sako et al., 2010), selectively reduces SMAD2/3 activation (supplementary material Fig. S4A,B; Ohsawa et al., 2006; Suragani et al., 2014; Zhou et al., 2010) and increases bone mass (Attie et al., 2013; Koncarevic et al., 2010). We reasoned that, if the reduced activin signaling underlies high bone mass in *Bmpr2*-cKO mice, then sequestration of activins with receptor decoy would have little or no additional effect on bone mass.

Table 1. Bone volume and mineral density of proximal tibiae from *Bmpr2*-floxed and *Bmpr2*-cKO mice

			Genotype			
Age of mice	Gender		*Bmpr2*-floxed	*Bmpr2*-cKO	Change (%)	*P* value
4 weeks	Male	BV/TV	0.0731±0.0028	0.0723±0.0036	−1.20	ns
		vBMD	71.11±7.531	72.90±6.541	2.50	ns
	Female	BV/TV	0.0673±0.0034	0.0769±0.0039	14.26	ns
		vBMD	68.20±6.040	84.31±6.613	23.62	ns
9 weeks	Male	BV/TV	0.1082±0.0092	0.1405±0.0054	29.85	0.0132
		vBMD	88.97±11.41	124.0±9.965	39.37	0.0432
	Female	BV/TV	0.0936±0.0073	0.1735±0.0108	85.36	<0.0001
		vBMD	75.28±7.357	164.5±10.87	118.51	<0.0001
15 weeks	Male	BV/TV	0.1341±0.0107	0.1835±0.0088	36.84	0.0024
		vBMD	128.4±12.33	185.3±10.29	44.31	0.0024
	Female	BV/TV	0.1004±0.0069	0.1522±0.0088	51.59	0.0009
		vBMD	95.52±8.975	155.9±11.25	63.21	0.0018

Change expressed as the percentage difference from gender-matched *Bmpr2*-floxed mice. n≥6 each group. BV/TV, bone volume/tissue volume; vBMD, volumetric bone mineral density expressed in mg hydroxyapatite per cubic centimeter; ns, not statistically significant.

Journal of Cell Science (2015) 128, 1308–1315 doi:10.1242/jcs.156737

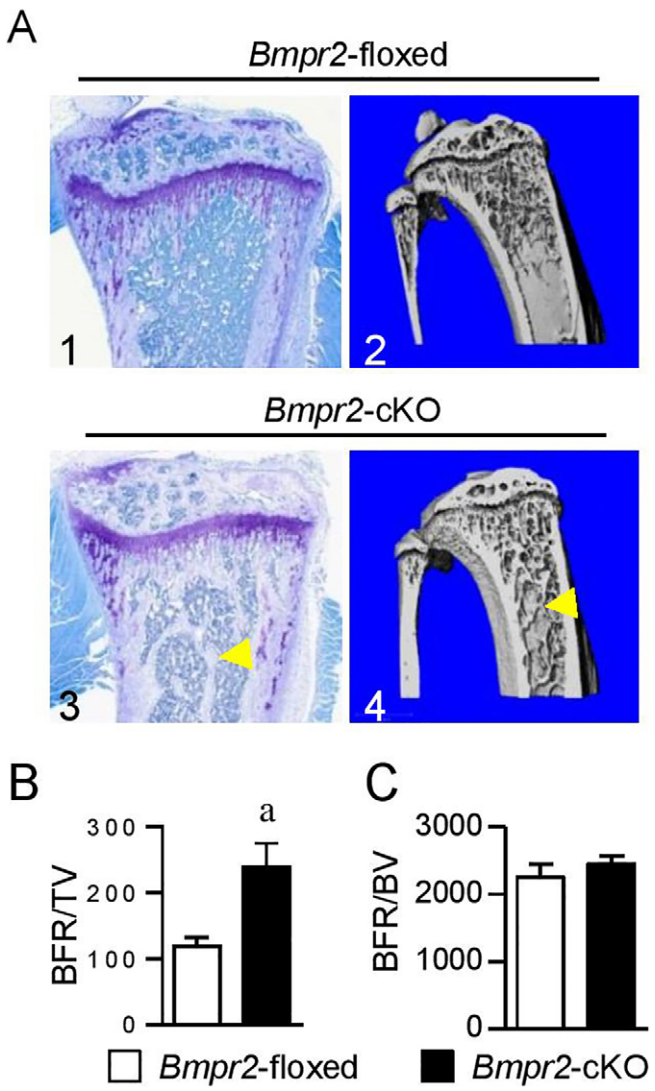

Fig. 3. High bone mass in *Bmpr2*-cKO mice due to increased bone formation rate. (A) Representative histological (1, 3) and μCT (2, 4) images of female 9-week-old *Bmpr2*-floxed (1, 2) and *Bmpr2*-cKO (3, 4) mice. The yellow arrowhead indicates increased trabecular bone volume in *Bmpr2*-cKO femur. (B,C) Histomorphometric analyses of 10-week-old *Bmpr2*-floxed and *Bmpr2*-cKO mice. $n \geq 8$ each group. BFR, bone formation rate; BV, bone volume; TV, tissue volume. $^{a}P<0.005$ compared with *Bmpr2*-floxed by Mann–Whitney test.

Consistent with previous reports where activin sequestration increased body weight gain and muscle mass (e.g. Cadena et al., 2010; Lee et al., 2012; Lee et al., 2005; Wang and McPherron, 2012), activin sequestration in *Bmpr2*-cKO mice increased the rate of body weight gain and the mass of the pectoralis major muscle (Fig. 4A,B), which are cellular targets outside the *Prx1*-Cre expression domain (Durland et al., 2008; Logan et al., 2002). In contrast, activin sequestration had a statistically indiscernible effect on trabecular bone mass and mineral density (Fig. 4C,D) in the tibiae of *Bmpr2*-cKO mice. This does not appear to be due to reduced activin ligand availability because the expression levels of activin ligands and their antagonists were unchanged in the bones of *Bmpr2*-cKO mice (supplementary material Fig. S3B); similarly, BMP ligand and antagonist expression levels were unaltered in *Bmpr2*-cKO bones (supplementary material Fig. S3B). The ability of the ACVR2B receptor decoy to substantially augment bone mass and mineral density as administered was simultaneously confirmed in a small cohort of *Bmpr2*-floxed mice (supplementary material Fig. S4E,F). The final bone mass and density attained after activin sequestration was the same in *Bmpr2*-floxed and *Bmpr2*-cKO mice, supporting the idea that impaired activin pathway activation underlies the bone phenotype we observe in *Bmpr2*-cKO mice.

DISCUSSION

Both BMPs and activins elicit pathway activation through interaction with heteromeric complexes containing type 1 and type 2 receptors (Zi et al., 2012). As represented in Fig. 5, structural differences mean that BMP ligands interact with BMP type 1 receptors (ALK1, ALK2, ALK3 and ALK6, also known as ACVRL1, ACVR1, BMPR1A and BMPR1B, respectively), whereas activin and related ligands (e.g. GDF8, GDF11) interact with activin type 1 receptors (ALK4 and ALK7, also known as ACVR1B and ACVR1C, respectively) (Hinck, 2012). This distinction stratifies the activation of SMAD1/5/8 versus SMAD2/3 downstream of BMPs and activins, respectively (Fig. 5A). Structural differences also govern interaction of ligands with type 2 receptors; only BMPs bind to the BMP-specific type 2 receptor BMPR2 and activate SMAD1/5/8 (Fig. 5A) (Hinck, 2012), whereas the type 2 receptors ACVR2A/B bind both BMPs and activins, engaging either SMAD1/5/8 or SMAD2/3, respectively (Fig. 5A) (Hinck, 2012). We hypothesized that BMPR2 is the preferred type 2 receptor for BMPs in bone, and that by removing BMPR2 from bone-forming cells we would create competition for a shared pool of ACVR2A/B molecules (Fig. 5B). Surprisingly, competition for ACVR2A/B led to a selective reduction in activin pathway signaling in bone with no apparent alteration in BMP signaling. The high bone mass phenotype we observed in *Bmpr2*-cKO mice is consistent with previous reports detailing the negative effect of activin on bone formation and matrix mineralization (Alves et al., 2013; Bialek et al., 2013; Eijken et al., 2007; Fajardo et al., 2010; Ikenoue et al., 1999; Koncarevic et al., 2010; Lotinun et al., 2010; Pearsall et al., 2008; Perrien et al., 2007; Ruckle et al., 2009; Sherman et al., 2013).

Collectively, our findings suggest that the availability of BMPR2 in bone-forming target cells provides a novel mechanism for establishing the relative amount of BMP to activin signaling. When BMPR2 is reduced or absent, increased BMP utilization of ACVR2A/B occurs at the expense of activin signaling. Although unexpected, this finding is supported by the fact that, in general, the affinity of BMPs for ACVR2A/B is in the same range as the affinity for BMPR2 (Allendorph et al., 2006; Berasi et al., 2011; Daly and Hearn, 2006; Greenwald et al., 2003; Greenwald et al., 2004; Heinecke et al., 2009; Hu et al., 2010; Isaacs et al., 2010; Kirsch et al., 2000; Knaus and Sebald, 2001; Koncarevic et al., 2010; Rosenzweig et al., 1995; Sako et al., 2010; Sengle et al., 2008), and BMPs also possess a flexible mode of receptor complex assembly, which might enhance their ability to compete with activins that have only a single mode of complex assembly (Hinck, 2012). Because bone cells have abundant type 1 BMP receptors (ALK2, ALK3 and ALK6, BioGPS Database), pre-formed receptor complexes might also be biased toward BMP binding. We do not believe our finding is only applicable to bone cells, as Piek et al. have reported that BMP7 can effectively compete with activin A for utilization of ACVR2A/B in human embryonic carcinoma cells (Piek et al., 1999), and direct competition for ACVR2A/B between BMP7 and the activin-like

Journal of Cell Science (2015) 128, 1308–1315 doi:10.1242/jcs.156737

Table 2. Histomorphometric analysis of *Bmpr2*-floxed and *Bmpr2*-cKO mice

Parameter	Genotype		Change (%)	*P* value
	Bmpr2-floxed	*Bmpr2*-cKO		
Osteoblast density (N.Ob/B.Pm, per mm)	10.78±1.180	12.06±2.478	11.87	0.6839
Osteoblast coverage (Ob.S/BS, %)	13.26±1.481	15.41±3.270	16.21	0.6040
Surface undergoing mineralization (MS/BS, %)	32.39±3.103	38.75±1.676	19.64	0.0658
Trabecular mineral apposition rate (MAR, μm/day)	2.871±0.1994	3.571±0.1978	24.38	0.0278
Trabecular bone formation rate (BFR/BS, $\mu m^3/\mu m^2$/day)	327.1±23.33	498.4±25.89	52.37	0.0002
Endocortical mineral apposition rate (MAR, μm/day)	0.97±0.36	2.25±0.19	131.96	0.0070
Osteoclast density (N.Oc/B.Pm, per mm)	1.327±0.2539	1.372±0.2945	3.39	0.9126
Osteoclast coverage (Oc.S/BS, %)	3.425±0.5214	3.321±0.6657	−3.04	0.9091
Surface undergoing erosion (ES/BS, %)	1.803±0.3247	1.453±0.3062	−19.41	0.4521

Change expressed as the percentage difference from *Bmpr2*-floxed mice. n ≥ 8 for each group and parameter. B.Pm, bone perimeter; BFR, bone formation rate; BS, bone surface; ES, eroded surface; MAR, mineral apposition rate; MS, mineralizing surface; N.Ob, number of osteoblasts; N.Oc, number of osteoclasts; Ob.S, osteoblast surface; Oc.S, osteoclast surface.

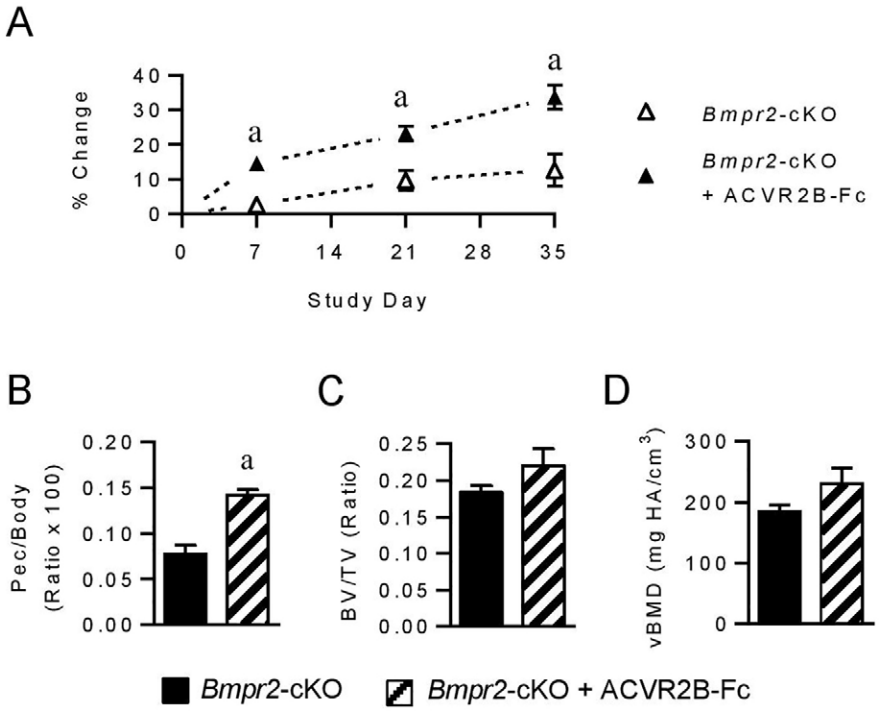

Fig. 4. Effects of activin receptor decoy administration in *Bmpr2*-cKO mice. (A) Rate of body weight gain over a 5-week ACVR2B-Fc treatment period in *Bmpr2*-cKO mice expressed as the mean percentage change from subject body weight on study day 0. (B–D) Effect of activin sequestration on dry weight of pectoralis major (B) and tibia trabecular bone volume (C) and bone mineral density (D) in *Bmpr2*-cKO mice. Data for untreated cohorts in C,D are also reported in Table 1. $n \geq 3$ for all groups. [a]$P<0.05$ compared with untreated *Bmpr2*-cKO.

ligand GDF8 has been reported by Rebbapragada et al. during adipogenesis (Rebbapragada et al., 2003).

Our model would predict that changes in either receptor or ligand availability (for instance, through altered expression or sequestration by extracellular antagonists) have the potential to modulate the balance of BMP versus activin signaling in a given cell. With respect to bone physiology, it is unknown whether the expression profile of type 2 BMP and activin receptors changes with age, but the ligands available to interact with type 2 BMP and activin receptors do change: BMP levels decline with age, which correlates with a decrease in ability to form new bone (Moerman et al., 2004; Syftestad and Urist, 1982), and there is a dramatic increase in circulating activin levels in adults of both genders, especially in the last decades of life (Baccarelli et al.,

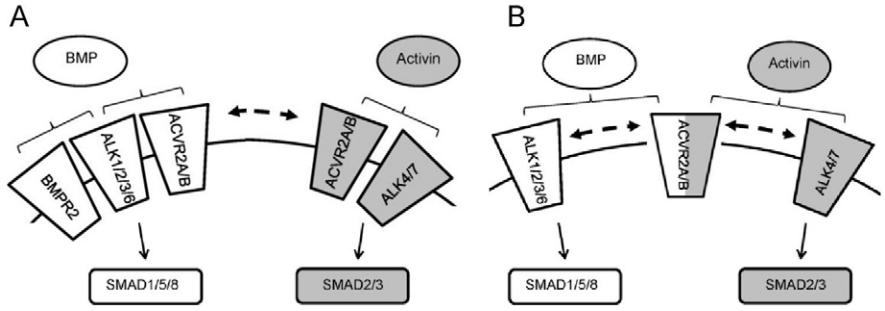

Fig. 5. Model of BMP and activin signaling. (A,B) Schematic of BMP and activin signaling in wild-type (A) and *Bmpr2*-cKO (B) cells. The type 2 receptors ACVR2A/B are shared between the BMP and activin pathways and elicit activation of either SMAD1/5/8 (in complex with the type 1 receptors ALK1, ALK2, ALK3 or ALK6) or SMAD2/3 (in complex with the type 1 receptors ALK4 or ALK7) in response to BMP or activin ligands, respectively (A). Removal of the type 2 receptor BMPR2 requires all BMP and activin signaling to utilize a common pool of ACVR2A/B molecules (B).

2001; Hurwitz and Santoro, 2004). In other contexts, serum immune-reactive activin is elevated further in patients with several diseases including hyperthyroidism, liver cirrhosis, chronic renal failure, advanced solid cancers, septicemia, acute inflammation and type 2 diabetes (de Kretser et al., 2011; Harada et al., 1996; Ueland et al., 2012). Our findings in bone raise the possibility that type 2 receptor segregation and/or competition could be a generalized mechanism by which BMP and activin signaling interact. Given that modulation of both BMP and activin pathways is of current clinical interest, a more detailed understanding of the molecular relationship between these pathways might provide insight into the development of new therapeutic strategies that are widely applicable.

MATERIALS AND METHODS

Mouse lines

The generation of the mouse lines used in this study, *Bmpr2*^{floxed} (Beppu et al., 2005), *Prx1*-Cre transgenic (Logan et al., 2002), and Rosa26$^{mT(mG)}$ Cre reporter mice (Muzumdar et al., 2007), have been described previously. For experimental study groups, female *Bmpr2*$^{floxed/floxed}$ mice were bred to male *Bmpr2*$^{floxed/floxed}$; *Prx1*-Cre mice to generate *Bmpr2* conditional knockout (*Bmpr2*-cKO) mice and Cre-negative *Bmpr2*$^{floxed/floxed}$ littermates (*Bmpr2*-floxed). Animals were killed by exposure to CO_2 followed by cervical dislocation. All animal experiments were performed under supervision of the Harvard Medical Area Standing Committee on Animals.

Osteoblast culture

Osteoblasts were isolated from the calvariae of newborn *Bmpr2*$^{floxed/floxed}$; *Rosa26*$^{mT(mG)}$ as described previously (Bakker and Klein-Nulend, 2003). Isolated cells were pooled to reduce technical variability, expanded and then split prior to delivery of adenovirus (Ad-CMV-Cre or Ad-CMV-Empty; Baylor College of Medicine Vector Development Lab, Houston, Texas, USA); recombination was monitored by expression of GFP from the *Rosa26*$^{mT(mG)}$ reporter. Cells were maintained in Dulbecco's modified Eagle's medium (DMEM) supplemented with 10% fetal bovine serum (FBS; Gibco, Life Technologies, Grand Island, New York, NY); for signaling studies, cells were serum-restricted in DMEM plus 2% FBS, treated with 100 ng/ml activin A (R&D Systems) for 1 hour, lysed and prepared for western blotting as described below.

Western blots

Western blotting was performed on protein isolates from primary osteoblasts and marrow-free femora lysed in RIPA lysis buffer supplemented with Halt Protease & Phosphatase Inhibitor Cocktail (Thermo, Waltham, MA). Prior to lysis, femora were cleaned of soft tissue, opened to expose the medullary cavity, centrifuged at 500 ***g*** for 2 minutes to separate marrow, and then homogenized using a Bullet Blender (Next Advance, Averill Park, New York, NY). Blotting was performed using antibodies against the following proteins: phosphorylated (phospho)-SMAD1/5/8 (Cell Signaling, Danvers, MA), phospho-SMAD2/3 (Cell Signaling), SMAD1 (Cell Signaling), SMAD2/3 (Cell Signaling), β-actin (Sigma-Aldrich, St. Louis, MO), mouse IgG conjugated to horseradish peroxidase (HRP; KPL, Gaithersburg, MD) and rabbit IgG conjugated to HRP (Cell Signaling). Blots were developed using SuperSignal West Femto Substrate (Thermo). For each time point, *Bmpr2*-floxed and *Bmpr2*-cKO samples were run on the same gels to avoid across-gel comparison and dashed lines are included to indicate where lanes are cropped to aid clarity of presentation. Signaling analyses were quantified by determining the ratio of the phosphorylated (active) SMAD isoform to the total pool. The validity of this approach is confirmed by the fact that total SMAD expression levels are unchanged relative to β-actin in *Bmpr2*-cKO mice (supplementary material Fig. S1C,D) or with ACVR2B-Fc treatment (supplementary material Fig. S1E). Band densities were quantified using ImageJ and normalized to *Bmpr2*-floxed control. Data are expressed as group mean±s.e.m. based on each individual ratio. Stripping of membranes was accomplished using Restore Western Blot Stripping Buffer (Thermo).

Physiological analysis of bones

Standard histomorphometric analyses were performed on the proximal tibiae of 10-week-old female mice. To examine mineral apposition rate, mice were injected intra-peritoneally with 20 µg calcein (Sigma-Aldrich) per gram body weight at 7 days and 2 days prior to killing. Tibiae were collected immediately following killing, fixed in 70% ethanol, embedded in methylmethacrylate without decalcification and sectioned. Parameters were examined by a blinded scorer. The reader is directed to an excellent guide to bone histomorphometry (Dempster et al., 2013).

For micro-computed tomography (µCT) analyses, bones were collected immediately after killing and fixed in 10% neutral buffered formalin (Millipore, Billerica, MA). Bones were exchanged into 70% ethanol, stored at 4℃, and analyzed at the HSDM µCT Core Facility on a SCANCO µCT 35 scanner. Bone volume and mineral density were determined using the following settings: FOV/diameter: 7168 µm; voxel size: 7.0 µm; slice increment: 7.0 µm; projections: 500; sample time: 600 ms; µ-scaling: 4096; energy: 55,000 V; intensity: 145 µA. The reader is directed to an excellent guide to µCT in rodents (Bouxsein et al., 2010).

Gene expression analyses

RNA was collected from isolated osteoblasts and marrow-free humerii from 4-week-old female or 15-week-old male mice using the RNEasy Plus Universal Kit (QIAGEN, Valencia, CA) after homogenization using a Bullet Blender (Next Advance). Reverse transcription was performed using an EcoDry Premix Kit (Clontech, Mountain View, CA). Quantitative PCR was performed using FastStart Universal SYBR Green Master Mix (Rox) (Roche, Nutley, NJ) on a StepOnePlus Real-Time PCR System (Applied Biosystems, Life Technologies) and primers as outlined in supplementary material Table S2. All primers were designed to cross exon boundaries and total RNA was treated with DNase. Data were analyzed by the comparative Ct method relative to cyclophilin B (*Ppib* Taqman probe, Mm00478295_m1, Life Technologies) using the equation $2^{-\Delta\Delta Ct}$.

ACVR2B receptor decoy administration

Recombinant human ACVR2B extracellular domain fused to human IgG1 Fc (ACVR2B-Fc) was obtained as a gift from Regeneron Pharmaceuticals (Tarrytown, New York, NY). Using the dosing scheme described by Koncarevic et al. (Koncarevic et al., 2010), male *Bmpr2*-floxed and *Bmpr2*-cKO littermates were treated with 10 µg ACVR2B-Fc in sterile PBS per gram body weight by intraperitoneal injection for time period indicated. Body weight was taken on day 0 and prior to each treatment. Upon killing, bones were processed for µCT as described above and the pectoralis major muscle was excised, dried at 37℃ for two days, then weighed.

Statistical analyses

All quantitative data are expressed as mean±s.e.m. except where indicated. Statistical significance was determined by unpaired Student's *t*-test for individual pairwise comparisons and one-way ANOVA with *post hoc* Newman–Keuls correction for multiple pairwise comparisons using GraphPad Prism (except where indicated). $P<0.05$ was considered significant.

Acknowledgements

We gratefully acknowledge John Martin (Harvard School of Dental Medicine) for µCT analyses and Regeneron Pharmaceuticals for the ACVR2B-Fc.

Competing interests

The authors declare no competing or financial interests.

Author contributions

J.W.L., G.I., L.G. and V.R. designed the study; J.W.L., G.I., S.L., V.S.S., S.O. and K.C. performed the experiments; all authors analyzed and interpreted the results; J.W.L. and V.R. wrote the manuscript; all authors read and approved the final version.

Funding
This study was supported by the National Institute of Arthritis and Musculoskeletal and Skin Diseases (NIAMS) [grant numbers R01AR055904 and R01AR064227 to V.R.]; the Harvard School of Dental Medicine Dean's Scholar Award issued to J.W.L. and G.I.; and Marian University intramural funds issued to J.W.L.
Deposited in PMC for release after 12 months.

Supplementary material
Supplementary material available online at
http://jcs.biologists.org/lookup/suppl/doi:10.1242/jcs.156737/-/DC1

References
Allendorph, G. P., Vale, W. W. and Choe, S. (2006). Structure of the ternary signaling complex of a TGF-beta superfamily member. *Proc. Natl. Acad. Sci. USA* **103**, 7643-7648.
Almeida, M., Iyer, S., Martin-Millan, M., Bartell, S. M., Han, L., Ambrogini, E., Onal, M., Xiong, J., Weinstein, R. S., Jilka, R. L. et al. (2013). Estrogen receptor-α signaling in osteoblast progenitors stimulates cortical bone accrual. *J. Clin. Invest.* **123**, 394-404.
Alves, R. D., Eijken, M., Bezstarosti, K., Demmers, J. A. and van Leeuwen, J. P. (2013). Activin A suppresses osteoblast mineralization capacity by altering extracellular matrix composition and impairing matrix vesicle production. *Mol. Cell. Proteomics* **12**, 2890-2900.
Attie, K. M., Borgstein, N. G., Yang, Y., Condon, C. H., Wilson, D. M., Pearsall, A. E., Kumar, R., Willins, D. A., Seehra, J. S. and Sherman, M. L. (2013). A single ascending-dose study of muscle regulator ACE-031 in healthy volunteers. *Muscle Nerve* **47**, 416-423.
Baccarelli, A., Morpurgo, P. S., Corsi, A., Vaghi, I., Fanelli, M., Cremonesi, G., Vaninetti, S., Beck-Peccoz, P. and Spada, A. (2001). Activin A serum levels and aging of the pituitary-gonadal axis: a cross-sectional study in middle-aged and elderly healthy subjects. *Exp. Gerontol.* **36**, 1403-1412.
Bakker, A. and Klein-Nulend, J. (2003). Osteoblast isolation from murine calvariae and long bones. *Methods Mol. Med.* **80**, 19-28.
Beppu, H., Lei, H., Bloch, K. D. and Li, E. (2005). Generation of a floxed allele of the mouse BMP type II receptor gene. *Genesis* **41**, 133-137.
Berasi, S. P., Varadarajan, U., Archambault, J., Cain, M., Souza, T. A., Abouzeid, A., Li, J., Brown, C. T., Dorner, A. J., Seeherman, H. J. et al. (2011). Divergent activities of osteogenic BMP2, and tenogenic BMP12 and BMP13 independent of receptor binding affinities. *Growth Factors* **29**, 128-139.
Bialek, P., Parkington, J., Li, X., Gavin, D., Wallace, C., Zhang, J., Root, A., Yan, G., Warner, L., Seeherman, H. J. et al. (2013). A myostatin and activin decoy receptor enhances bone formation in mice. *Bone* **60**,162-171.
Bouxsein, M. L., Boyd, S. K., Christiansen, B. A., Guldberg, R. E., Jepsen, K. J. and Muller, R. (2010). Guidelines for assessment of bone microstructure in rodents using micro-computed tomography. *J. Bone Miner. Res.* **25**, 1468-1486.
Cadena, S. M., Tomkinson, K. N., Monnell, T. E., Spaits, M. S., Kumar, R., Underwood, K. W., Pearsall, R. S. and Lachey, J. L. (2010). Administration of a soluble activin type IIB receptor promotes skeletal muscle growth independent of fiber type. *J. Appl. Physiol.* **109**, 635-642.
Candia, A. F., Watabe, T., Hawley, S. H., Onichtchouk, D., Zhang, Y., Derynck, R., Niehrs, C. and Cho, K. W. (1997). Cellular interpretation of multiple TGF-beta signals: intracellular antagonism between activin/BVg1 and BMP-2/4 signaling mediated by Smads. *Development* **124**, 4467-4480.
Daly, R. and Hearn, M. T. (2006). Expression of the human activin type I and II receptor extracellular domains in Pichia pastoris. *Protein Expr. Purif.* **46**, 456-467.
de Kretser, D. M., O'Hehir, R. E., Hardy, C. L. and Hedger, M. P. (2011). The roles of activin A and its binding protein, follistatin, in inflammation and tissue repair. *Mol. Cell. Endocrinol.* **359**, 101-106.
Dempster, D. W., Compston, J. E., Drezner, M. K., Glorieux, F. H., Kanis, J. A., Malluche, H., Meunier, P. J., Ott, S. M., Recker, R. R. and Parfitt, A. M. (2013). Standardized nomenclature, symbols, and units for bone histomorphometry: a 2012 update of the report of the ASBMR Histomorphometry Nomenclature Committee. *J. Bone Miner. Res.* **28**, 2-17.
Durland, J. L., Sferlazzo, M., Logan, M. and Burke, A. C. (2008). Visualizing the lateral somitic frontier in the Prx1Cre transgenic mouse. *J. Anat.* **212**, 590-602.
Eijken, M., Swagemakers, S., Koedam, M., Steenbergen, C., Derkx, P., Uitterlinden, A. G., van der Spek, P. J., Visser, J. A., de Jong, F. H., Pols, H. A. et al. (2007). The activin A-follistatin system: potent regulator of human extracellular matrix mineralization. *FASEB J.* **21**, 2949-2960.
Fajardo, R. J., Manoharan, R. K., Pearsall, R. S., Davies, M. V., Marvell, T., Monnell, T. E., Ucran, J. A., Pearsall, A. E., Khanzode, D., Kumar, R. et al. (2010). Treatment with a soluble receptor for activin improves bone mass and structure in the axial and appendicular skeleton of female cynomolgus macaques (Macaca fascicularis). *Bone* **46**, 64-71.
Gamer, L. W., Tsuji, K., Cox, K., Capelo, L. P., Lowery, J., Beppu, H. and Rosen, V. (2011). BMPR-II is dispensable for formation of the limb skeleton. *Genesis* **49**, 719-724.
Goumans, M. J., Lebrin, F. and Valdimarsdottir, G. (2003). Controlling the angiogenic switch: a balance between two distinct TGF-b receptor signaling pathways. *Trends Cardiovasc. Med.* **13**, 301-307.
Greenwald, J., Groppe, J., Gray, P., Wiater, E., Kwiatkowski, W., Vale, W. and Choe, S. (2003). The BMP7/ActRII extracellular domain complex provides new insights into the cooperative nature of receptor assembly. *Mol. Cell* **11**, 605-617.
Greenwald, J., Vega, M. E., Allendorph, G. P., Fischer, W. H., Vale, W. and Choe, S. (2004). A flexible activin explains the membrane-dependent cooperative assembly of TGF-beta family receptors. *Mol. Cell* **15**, 485-489.
Han, C., Hong, K. H., Kim, Y. H., Kim, M. J., Song, C., Kim, M. J., Kim, S. J., Raizada, M. K. and Oh, S. P. (2013). SMAD1 deficiency in either endothelial or smooth muscle cells can predispose mice to pulmonary hypertension. *Hypertension* **61**, 1044-1052.
Harada, K., Shintani, Y., Sakamoto, Y., Wakatsuki, M., Shitsukawa, K. and Saito, S. (1996). Serum immunoreactive activin A levels in normal subjects and patients with various diseases. *J. Clin. Endocrinol. Metab.* **81**, 2125-2130.
Heinecke, K., Seher, A., Schmitz, W., Mueller, T. D., Sebald, W. and Nickel, J. (2009). Receptor oligomerization and beyond: a case study in bone morphogenetic proteins. *BMC Biol.* **7**, 59.
Hinck, A. P. (2012). Structural studies of the TGF-βs and their receptors – insights into evolution of the TGF-β superfamily. *FEBS Lett.* **586**, 1860-1870.
Hu, J., Duppatla, V., Harth, S., Schmitz, W. and Sebald, W. (2010). Site-specific PEGylation of bone morphogenetic protein-2 cysteine analogues. *Bioconjug. Chem.* **21**, 1762-1772.
Hurwitz, J. M. and Santoro, N. (2004). Inhibins, activins, and follistatin in the aging female and male. *Semin. Reprod. Med.* **22**, 209-217.
Ikenoue, T., Jingushi, S., Urabe, K., Okazaki, K. and Iwamoto, Y. (1999). Inhibitory effects of activin-A on osteoblast differentiation during cultures of fetal rat calvarial cells. *J. Cell. Biochem.* **75**, 206-214.
Isaacs, M. J., Kawakami, Y., Allendorph, G. P., Yoon, B. H., Izpisua Belmonte, J. C. and Choe, S. (2010). Bone morphogenetic protein-2 and -6 heterodimer illustrates the nature of ligand-receptor assembly. *Mol. Endocrinol.* **24**, 1469-1477.
Izumi, N., Mizuguchi, S., Inagaki, Y., Saika, S., Kawada, N., Nakajima, Y., Inoue, K., Suehiro, S., Friedman, S. L. and Ikeda, K. (2006). BMP-7 opposes TGF-beta1-mediated collagen induction in mouse pulmonary myofibroblasts through Id2. *Am. J. Physiol.* **290**, L120-L126.
Kirsch, T., Nickel, J. and Sebald, W. (2000). BMP-2 antagonists emerge from alterations in the low-affinity binding epitope for receptor BMPR-II. *EMBO J.* **19**, 3314-3324.
Knaus, P. and Sebald, W. (2001). Cooperativity of binding epitopes and receptor chains in the BMP/TGFbeta superfamily. *Biol. Chem.* **382**, 1189-1195.
Kolanczyk, M., Kossler, N., Kühnisch, J., Lavitas, L., Stricker, S., Wilkening, U., Manjubala, I., Fratzl, P., Spörle, R., Herrmann, B. G. et al. (2007). Multiple roles for neurofibromin in skeletal development and growth. *Hum. Mol. Genet.* **16**, 874-886.
Koncarevic, A., Cornwall-Brady, M., Pullen, A., Davies, M., Sako, D., Liu, J., Kumar, R., Tomkinson, K., Baker, T., Umiker, B. et al. (2010). A soluble activin receptor type IIb prevents the effects of androgen deprivation on body composition and bone health. *Endocrinology* **151**, 4289-4300.
Koncarevic, A., Kajimura, S., Cornwall-Brady, M., Andreucci, A., Pullen, A., Sako, D., Kumar, R., Grinberg, A. V., Liharska, K., Ucran, J. A. et al. (2012). A novel therapeutic approach to treating obesity through modulation of TGFβ signaling. *Endocrinology* **153**, 3133-3146.
Lee, S. J., Reed, L. A., Davies, M. V., Girgenrath, S., Goad, M. E., Tomkinson, K. N., Wright, J. F., Barker, C., Ehrmantraut, G., Holmstrom, J. et al. (2005). Regulation of muscle growth by multiple ligands signaling through activin type II receptors. *Proc. Natl. Acad. Sci. USA* **102**, 18117-18122.
Lee, S. J., Huynh, T. V., Lee, Y. S., Sebald, S. M., Wilcox-Adelman, S. A., Iwamori, N., Lepper, C., Matzuk, M. M. and Fan, C. M. (2012). Role of satellite cells versus myofibers in muscle hypertrophy induced by inhibition of the myostatin/activin signaling pathway. *Proc. Natl. Acad. Sci. USA* **109**, E2353-E2360.
Li, S., Meyer, N. P., Quarto, N. and Longaker, M. T. (2013). Integration of multiple signaling regulates through apoptosis the differential osteogenic potential of neural crest-derived and mesoderm-derived Osteoblasts. *PLoS ONE* **8**, e58610.
Liu, H., Zhang, R., Chen, D., Oyajobi, B. O. and Zhao, M. (2012). Functional redundancy of type II BMP receptor and type IIB activin receptor in BMP2-induced osteoblast differentiation. *J. Cell. Physiol.* **227**, 952-963.
Logan, M., Martin, J. F., Nagy, A., Lobe, C., Olson, E. N. and Tabin, C. J. (2002). Expression of Cre Recombinase in the developing mouse limb bud driven by a Prxl enhancer. *Genesis* **33**, 77-80.
Lotinun, S., Pearsall, R. S., Davies, M. V., Marvell, T. H., Monnell, T. E., Ucran, J., Fajardo, R. J., Kumar, R., Underwood, K. W., Seehra, J. et al. (2010). A soluble activin receptor Type IIA fusion protein (ACE-011) increases bone mass via a dual anabolic-antiresorptive effect in Cynomolgus monkeys. *Bone* **46**, 1082-1088.
Lowery, J. W. and de Caestecker, M. P. (2010). BMP signaling in vascular development and disease. *Cytokine Growth Factor Rev.* **21**, 287-298.
Massagué, J. (2012). TGFβ signalling in context. *Nat. Rev. Mol. Cell Biol.* **13**, 616-630.
Matsumoto, Y., Otsuka, F., Hino, J., Miyoshi, T., Takano, M., Miyazato, M., Makino, H. and Kangawa, K. (2012). Bone morphogenetic protein-3b (BMP-3b) inhibits osteoblast differentiation via Smad2/3 pathway by counteracting Smad1/5/8 signaling. *Mol. Cell. Endocrinol.* **350**, 78-86.
Mishina, Y., Starbuck, M. W., Gentile, M. A., Fukuda, T., Kasparcova, V., Seedor, J. G., Hanks, M. C., Amling, M., Pinero, G. J., Harada, S. et al. (2004). Bone morphogenetic protein type IA receptor signaling regulates postnatal osteoblast function and bone remodeling. *J. Biol. Chem.* **279**, 27560-27566.

Moerman, E. J., Teng, K., Lipschitz, D. A. and Lecka-Czernik, B. (2004). Aging activates adipogenic and suppresses osteogenic programs in mesenchymal marrow stroma/stem cells: the role of PPAR-gamma2 transcription factor and TGF-beta/BMP signaling pathways. *Aging Cell* **3**, 379-389.
Morrell, N. W., Yang, X., Upton, P. D., Jourdan, K. B., Morgan, N., Sheares, K. K. and Trembath, R. C. (2001). Altered growth responses of pulmonary artery smooth muscle cells from patients with primary pulmonary hypertension to transforming growth factor-β(1) and bone morphogenetic proteins. *Circulation* **104**, 790-795.
Muzumdar, M. D., Tasic, B., Miyamichi, K., Li, L. and Luo, L. (2007). A global double-fluorescent Cre reporter mouse. *Genesis* **45**, 593-605.
Nguyen, T. Q. and Goldschmeding, R. (2008). Bone morphogenetic protein-7 and connective tissue growth factor: novel targets for treatment of renal fibrosis? *Pharm. Res.* **25**, 2416-2426.
Nicks, K. M., Perrien, D. S., Akel, N. S., Suva, L. J. and Gaddy, D. (2009). Regulation of osteoblastogenesis and osteoclastogenesis by the other reproductive hormones, Activin and Inhibin. *Mol. Cell. Endocrinol.* **310**, 11-20.
Ohsawa, Y., Hagiwara, H., Nakatani, M., Yasue, A., Moriyama, K., Murakami, T., Tsuchida, K., Noji, S. and Sunada, Y. (2006). Muscular atrophy of caveolin-3-deficient mice is rescued by myostatin inhibition. *J. Clin. Invest.* **116**, 2924-2934.
Oshimori, N. and Fuchs, E. (2012). Paracrine TGF-β signaling counterbalances BMP-mediated repression in hair follicle stem cell activation. *Cell Stem Cell* **10**, 63-75.
Pearsall, R. S., Canalis, E., Cornwall-Brady, M., Underwood, K. W., Haigis, B., Ucran, J., Kumar, R., Pobre, E., Grinberg, A., Werner, E. D. et al. (2008). A soluble activin type IIA receptor induces bone formation and improves skeletal integrity. *Proc. Natl. Acad. Sci. USA* **105**, 7082-7087.
Perrien, D. S., Akel, N. S., Edwards, P. K., Carver, A. A., Bendre, M. S., Swain, F. L., Skinner, R. A., Hogue, W. R., Nicks, K. M., Pierson, T. M. et al. (2007). Inhibin A is an endocrine stimulator of bone mass and strength. *Endocrinology* **148**, 1654-1665.
Piek, E., Afrakhte, M., Sampath, K., van Zoelen, E. J., Heldin, C. H. and ten Dijke, P. (1999). Functional antagonism between activin and osteogenic protein-1 in human embryonal carcinoma cells. *J. Cell. Physiol.* **180**, 141-149.
Rebbapragada, A., Benchabane, H., Wrana, J. L., Celeste, A. J. and Attisano, L. (2003). Myostatin signals through a transforming growth factor beta-like signaling pathway to block adipogenesis. *Mol. Cell. Biol.* **23**, 7230-7242.
Rosenzweig, B. L., Imamura, T., Okadome, T., Cox, G. N., Yamashita, H., ten Dijke, P., Heldin, C. H. and Miyazono, K. (1995). Cloning and characterization of a human type II receptor for bone morphogenetic proteins. *Proc. Natl. Acad. Sci. USA* **92**, 7632-7636.
Ruckle, J., Jacobs, M., Kramer, W., Pearsall, A. E., Kumar, R., Underwood, K. W., Seehra, J., Yang, Y., Condon, C. H. and Sherman, M. L. (2009). Single-dose, randomized, double-blind, placebo-controlled study of ACE-011 (ActRIIA-IgG1) in postmenopausal women. *J. Bone Miner. Res.* **24**, 744-752.
Saitoh, M., Shirakihara, T., Fukasawa, A., Horiguchi, K., Sakamoto, K., Sugiya, H., Beppu, H., Fujita, Y., Morita, I., Miyazono, K. et al. (2013). Basolateral BMP signaling in polarized epithelial cells. *PLoS ONE* **8**, e62659.
Sakai, R., Eto, Y., Hirafuji, M. and Shinoda, H. (2000). Activin release from bone coupled to bone resorption in organ culture of neonatal mouse calvaria. *Bone* **26**, 235-240.
Sako, D., Grinberg, A. V., Liu, J., Davies, M. V., Castonguay, R., Maniatis, S., Andreucci, A. J., Pobre, E. G., Tomkinson, K. N., Monnell, T. E. et al. (2010). Characterization of the ligand binding functionality of the extracellular domain of activin receptor type IIb. *J. Biol. Chem.* **285**, 21037-21048.
Sartori, R., Schirwis, E., Blaauw, B., Bortolanza, S., Zhao, J., Enzo, E., Stantzou, A., Mouisel, E., Toniolo, L., Ferry, A. et al. (2013). BMP signaling controls muscle mass. *Nat. Genet.* **45**, 1309-1318.
Sengle, G., Ono, R. N., Lyons, K. M., Bächinger, H. P. and Sakai, L. Y. (2008). A new model for growth factor activation: type II receptors compete with the prodomain for BMP-7. *J. Mol. Biol.* **381**, 1025-1039.
Sherman, M. L., Borgstein, N. G., Mook, L., Wilson, D., Yang, Y., Chen, N., Kumar, R., Kim, K. and Laadem, A. (2013). Multiple-dose, safety, pharmacokinetic, and pharmacodynamic study of sotatercept (ActRIIA-IgG1), a novel erythropoietic agent, in healthy postmenopausal women. *J. Clin. Pharmacol.* **53**, 1121-1130.
Simic, P., Culej, J. B., Orlic, I., Grgurevic, L., Draca, N., Spaventi, R. and Vukicevic, S. (2006). Systemically administered bone morphogenetic protein-6 restores bone in aged ovariectomized rats by increasing bone formation and suppressing bone resorption. *J. Biol. Chem.* **281**, 25509-25521.
Stumm, C. L., Halcsik, E., Landgraf, R. G., Camara, N. O., Sogayar, M. C. and Jancar, S. (2014). Lung remodeling in a mouse model of asthma involves a balance between TGF-β1 and BMP-7. *PLoS ONE* **9**, e95959.
Suragani, R. N., Cadena, S. M., Cawley, S. M., Sako, D., Mitchell, D., Li, R., Davies, M. V., Alexander, M. J., Devine, M., Loveday, K. S. et al. (2014). Transforming growth factor-β superfamily ligand trap ACE-536 corrects anemia by promoting late-stage erythropoiesis. *Nat. Med.* **20**, 408-414.
Syftestad, G. T. and Urist, M. R. (1982). Bone aging. *Clin. Orthop. Relat. Res.* **162**, 288-297.
Ueland, T., Aukrust, P., Aakhus, S., Smith, C., Endresen, K., Birkeland, K. I., Gullestad, L. and Johansen, O. E. (2012). Activin A and cardiovascular disease in type 2 diabetes mellitus. *Diab. Vasc. Dis. Res.* **9**, 234-237.
Wang, Q. and McPherron, A. C. (2012). Myostatin inhibition induces muscle fibre hypertrophy prior to satellite cell activation. *J. Physiol.* **590**, 2151-2165.
Winbanks, C. E., Chen, J. L., Qian, H., Liu, Y., Bernardo, B. C., Beyer, C., Watt, K. I., Thomson, R. E., Connor, T., Turner, B. J. et al. (2013). The bone morphogenetic protein axis is a positive regulator of skeletal muscle mass. *J. Cell Biol.* **203**, 345-357.
Wordinger, R. J., Fleenor, D. L., Hellberg, P. E., Pang, I. H., Tovar, T. O., Zode, G. S., Fuller, J. A. and Clark, A. F. (2007). Effects of TGF-beta2, BMP-4, and gremlin in the trabecular meshwork: implications for glaucoma. *Invest. Ophthalmol. Vis. Sci.* **48**, 1191-1200.
Yamamoto, M., Beppu, H., Takaoka, K., Meno, C., Li, E., Miyazono, K. and Hamada, H. (2009). Antagonism between Smad1 and Smad2 signaling determines the site of distal visceral endoderm formation in the mouse embryo. *J. Cell Biol.* **184**, 323-334.
Zhang, F., Qiu, T., Wu, X., Wan, C., Shi, W., Wang, Y., Chen, J. G., Wan, M., Clemens, T. L. and Cao, X. (2009). Sustained BMP signaling in osteoblasts stimulates bone formation by promoting angiogenesis and osteoblast differentiation. *J. Bone Miner. Res.* **24**, 1224-1233.
Zhao, M., Harris, S. E., Horn, D., Geng, Z., Nishimura, R., Mundy, G. R. and Chen, D. (2002). Bone morphogenetic protein receptor signaling is necessary for normal murine postnatal bone formation. *J. Cell Biol.* **157**, 1049-1060.
Zhao, L., Yee, M. and O'Reilly, M. A. (2013). Transdifferentiation of alveolar epithelial type II to type I cells is controlled by opposing TGF-β and BMP signaling. *Am. J. Physiol.* **305**, L409-L418.
Zhou, X., Wang, J. L., Lu, J., Song, Y., Kwak, K. S., Jiao, Q., Rosenfeld, R., Chen, Q., Boone, T., Simonet, W. S. et al. (2010). Reversal of cancer cachexia and muscle wasting by ActRIIB antagonism leads to prolonged survival. *Cell* **142**, 531-543.
Zi, Z., Chapnick, D. A. and Liu, X. (2012). Dynamics of TGF-β/Smad signaling. *FEBS Lett.* **586**, 1921-1928.
Zode, G. S., Clark, A. F. and Wordinger, R. J. (2009). Bone morphogenetic protein 4 inhibits TGF-beta2 stimulation of extracellular matrix proteins in optic nerve head cells: role of gremlin in ECM modulation. *Glia* **57**, 755-766.

Fig. S1 SMAD1/5/8 and SMAD2/3 in bones of *Bmpr2*-cKO mice. A: Western blots for phosphorylated isoforms of SMAD1/5/8 (pS1/5/8) and SMAD2/3 (pS2/3) relative to total SMAD1 or SMAD2. Lysates are from marrow-free femora of male mice at 4 weeks of age. Densitometry are normalized to *Bmpr2*-floxed from n=3 each genotype. Vertical bars indicate removal of intervening lane(s) so that samples most representative of group mean are shown. B: Western blot for SMAD1/5/8 activation in bones of *Bmpr2*-cKO mice at 9 weeks of age showing the intervening lane that was cropped so that samples most representative of group mean could be shown in Fig. 1D. **C-D:** SMAD1 and SMAD2 expression levels in bones of *Bmpr2*-cKO mice at 4 and 9 weeks of age. Western blots and densitometry for total SMAD1 or SMAD2 relative to β-actin. Lysates are from marrow-free femora of male mice at 4 weeks of age (C) and female mice at 9 weeks of age (D). Densitometry are normalized to *Bmpr2*-floxed from n≥3 each genotype. **E:** SMAD1 and SMAD2 expression levels in bones of ACVR2B-Fc treated mice at 9 weeks of age. Western blots and densitometry for total SMAD1 or SMAD2 relative to β-actin. Lysates are from marrow-free femora of *Bmpr2*-floxed mice two days after ACVR2B-Fc administration. Densitometry are normalized to untreated *Bmpr2*-floxed from n≥2 each genotype.

Fig. S2 A: Quantitative RT-PCR for Activin subunits (*Inhba* and *Inhbb)* and antagonists (*Inhibin* (*Inha*) and *Follistatin*) in *Bmpr2*-cKO osteoblasts. n=4 per genotype for all analyses. No statistically significant change in expression level of the queried genes was observed. **B:** Activin-responsiveness in *Bmpr2*-cKO osteoblasts. Western blot for phosphorylated isoforms of SMAD2/3 (pS2/3) relative to total SMAD2 in *Bmpr2*-floxed (Control) and *Bmpr2*-cKO (CMV-Cre) osteoblasts +/- 100 ng/ml Activin A treatment for 1 hour. β-actin expression serves a loading control.

Fig. S3 A: Quantitative RT-PCR for bone marker expression in marrow-free humerii of 4-week-old *Bmpr2*-floxed and *Bmpr2*-cKO mice. n≥4 per genotype for all analyses. No statistically significant change in expression level of the queried genes was observed. **B:** Quantitative RT-PCR for Activin ligands, BMP ligands, and antagonists in marrow-free humerii of 15-week-old *Bmpr2*-floxed and *Bmpr2*-cKO mice. n≥4 per genotype for all analyses. No statistically significant change in expression level of the queried genes was observed.

Fig. S4 Effects of Activin receptor decoy administration in *Bmpr2*-floxed mice. A-B. Western blots for phosphorylated isoforms of SMAD2/3 (A, pS2/3) and SMAD1/5/8 (B, pS1/5/8) relative to total SMAD2 or SMAD1. Lysates are from marrow-free femora of *Bmpr2*-floxed mice two days after ACVR2B-Fc administration. Vertical bar in B indicates removal of intervening lane so that samples most representative of group mean are shown. **C:** Rate of body weight gain over 5-week ACVR2B-Fc treatment period in *Bmpr2*-floxed mice expressed as mean percent change from subject body weight on study day 0. **D-F:** Effect of Activin sequestration on dry weight of pectoralis major (D) and tibia trabecular bone volume (E) and bone mineral density (F) in *Bmpr2*-floxed mice. Data for untreated cohorts in E-F are also reported in Table 1. $n \geq 2$ for all groups.

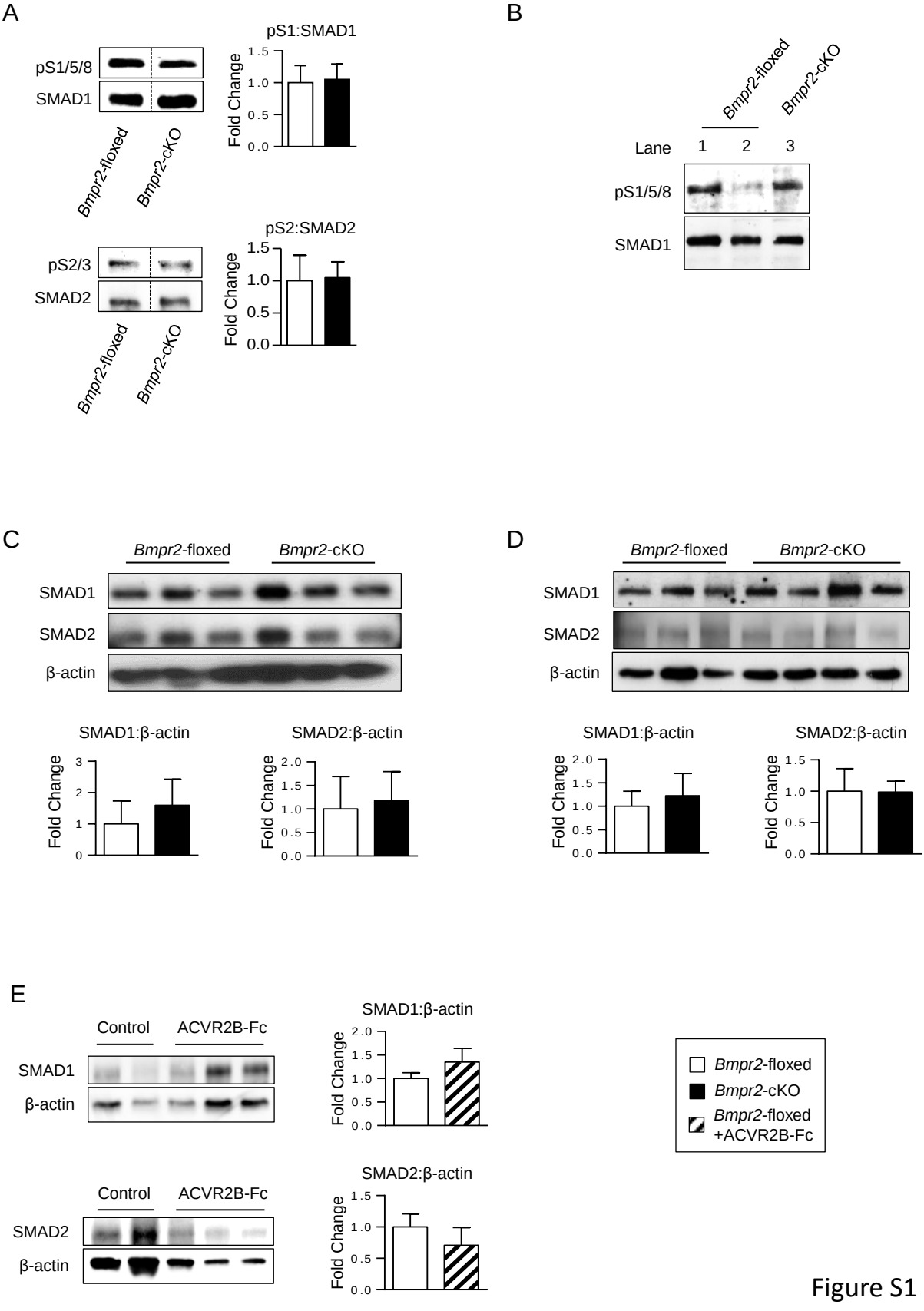
A
pS1:SMAD1
pS1/5/8
SMAD1
Bmpr2-floxed
Bmpr2-cKO
Fold Change
1.5
1.0
0.5
0.0
pS2:SMAD2
pS2/3
SMAD2
B
Bmpr2-floxed
Bmpr2-cKO
Lane
1
2
3
C
Bmpr2-floxed
Bmpr2-cKO
SMAD1
SMAD2
β-actin
SMAD1:β-actin
SMAD2:β-actin
D
E
Control
ACVR2B-Fc
Bmpr2-floxed
Bmpr2-cKO
Bmpr2-floxed
+ACVR2B-Fc

Figure S1

A

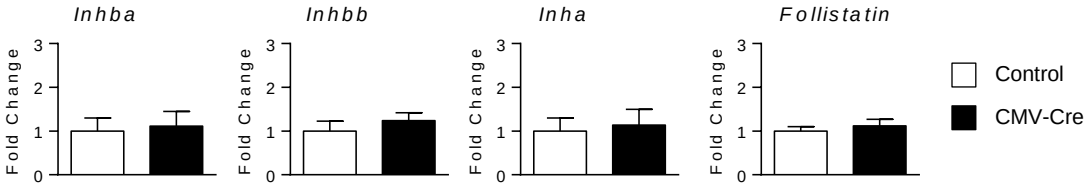
Inhba
Inhbb
Inha
Follistatin
Fold Change
0
1
2
3
Control
CMV-Cre

B

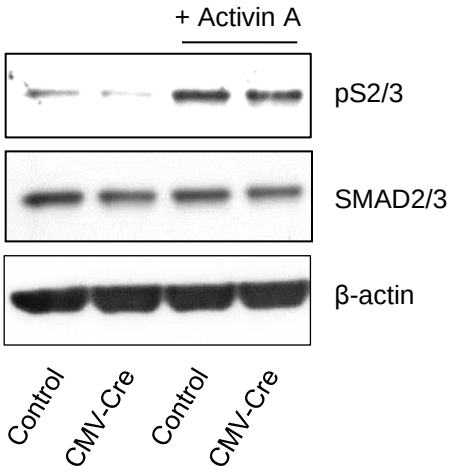
+ Activin A
pS2/3
SMAD2/3
β-actin
Control
CMV-Cre
Control
CMV-Cre

Figure S2

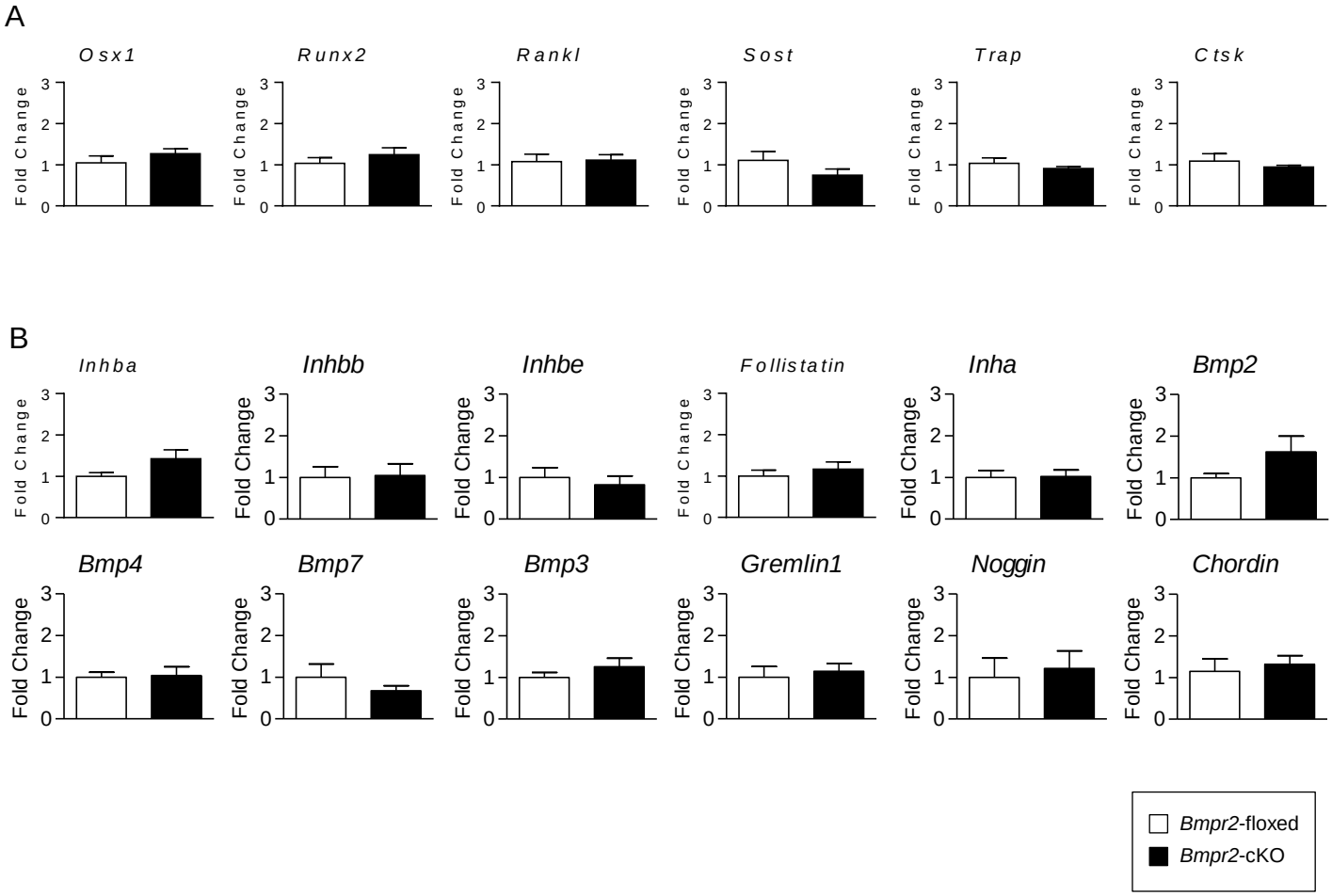
A
Osx1
Runx2
Rankl
Sost
Trap
Ctsk
Fold Change
B
Inhba
Inhbb
Inhbe
Follistatin
Inha
Bmp2
Bmp4
Bmp7
Bmp3
Gremlin1
Noggin
Chordin
Bmpr2-floxed
Bmpr2-cKO

Figure S3

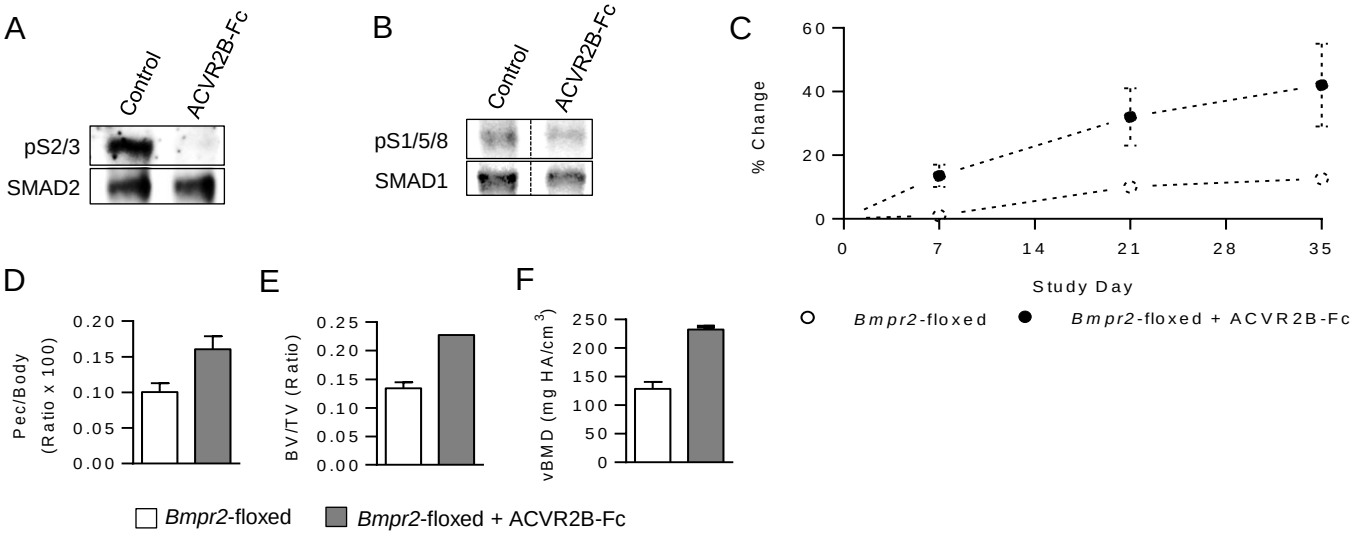
A
Control
ACVR2B-Fc
pS2/3
SMAD2
B
Control
ACVR2B-Fc
pS1/5/8
SMAD1
C
% Change
60
40
20
0
0
7
14
21
28
35
Study Day
Bmpr2-floxed
Bmpr2-floxed + ACVR2B-Fc
D
Pec/Body (Ratio x 100)
0.20
0.15
0.10
0.05
0.00
E
BV/TV (Ratio)
0.25
0.20
0.15
0.10
0.05
0.00
F
vBMD (mg HA/cm3)
250
200
150
100
50
0
Bmpr2-floxed
Bmpr2-floxed + ACVR2B-Fc

Figure S4

Table S1. μCT analyses of L5 vertebrae from 9-week-old *Bmpr2*-floxed and *Bmpr2*-cKO mice.

		Bmpr2-floxed	*Bmpr2*-cKO	*p* value
BV/TV	Male	0.2598±0.01333 (n=6)	0.2294±0.01572 (n=6)	0.1702
	Female	0.2209±0.01348 (n=3)	0.2362±0.00892 (n=5)	0.3591
Tb.Th (mm)	Male	0.04597±0.0006535 (n=6)	0.04357±0.001912 (n=6)	0.2624
	Female	0.04707±0.002202 (n=3)	0.04706±0.0004007 (n=5)	0.9970

Number of animals for each group indicated by (n). BV: bone volume, TV: tissue volume, Tb.Th: trabecular thickness.

Table S2. Sequences of primers used for RT-PCR analyses.

Target mRNA	Forward Primer	Reverse Primer
Acvr2a	GCAATGGCTTCAACCCTAGT	CCCTCCTGTACTTGTTCCTACTCA
Acvr2b	GGCCATGTACCGTCTGGT	TGGCTGTTCGGTTTGAGC
Bmpr2	GAGCCCTCCCTTGACCTG	GTATCGACCCCGTCCAATC
Bmp2	AGATCTGTACCGCAGGCACT	GTTCCTCCACGGCTTCTTC
Bmp4	GAGGAGTTTCCATCACGAAGA	GCTCTGCCGAGGAGATCA
Bmp7	CGAGACCTTCCAGATCACAGT	CAGCAAGAAGAGGTCCGACT
Bmp3	TCTCCCAAGTCATTTGATGCT	GCGTGATTTGATGGTTTCAA
Chordin	TCACTGCCCACCTCCTTG	GATCTTTTACCACGCCCTGA
Ctsk	AGCGAACAGATTCTCAACAGC	AGACAGAGCAAAGCTCACCAT
Follistatin	AAGCATTCTGGATCTTGCAACT	GATAGGAAAGCTGTAGTCCTGGTC
Hprt	CCTGCTGGATTACATTAAAGCACTG	GTCAAGGGCATATCCAACAACAAAC
Inha	GGAAGATGTCTCCCAGGCTA	TGGCTGGTCCTCACAGGT
Inhba	ATCATCACCTTTGCCGAGTC	TCACTGCCTTCCTTGGAAAT
Inhbb	GATCATCAGCTTTGCAGAGACA	TGCCTTCATTAGAGACGAAGAA
Inhbe	CATCAGCTTTGCTACCATCATAGA	AGGTGGTGGGACCAAAGAG
Noggin	TGATGGATCCCCACCAAC	CGCTAGAGGGTGGTGAAACT
Osx1	AGAGATCTGAGCTGGGTAGAGG	AAGAGAGCCTGGCAAGAGG
Phex	AGCGCTATGATTCCCCAGT	TTCAAGTGTGGGTAGAGTCTGG
Rankl	AGCCATTTGCACACCTCAC	CGTGGTACCAAGAGGACAGAGT
Runx2	CCACAAGGACAGAGTCAGATTACA	TGGCTCAGATAGGAGGGGTA
Sost	TCCTGAGAACAACCAGACCA	GCAGCTGTACTCGGACACATC
Trap	CGTCTCTGCACAGATTGCAT	AAGCGCAAACGGTAGTAAGG